Optics and Laser Technology 103 (2018) 300–310

Contents lists available at ScienceDirect

Optics and Laser Technology

journal homepage: www.elsevier.com/locate/optlastec

Full length article

Optimizing pulsed Nd:YAG laser beam welding process parameters to attain maximum ultimate tensile strength for thin AISI316L sheet using response surface methodology and simulated annealing algorithm

Amir Torabi, Farhad Kolahan *

Ferdowsi University of Mashhad, Department of Mechanical Engineering, P.O. Box 91775-1111, Mashhad, Iran

ARTICLE INFO

Article history:
Received 2 December 2017
Accepted 23 December 2017

Keywords:
Pulsed laser welding
Response Surface Methodology (RSM)
Regression modeling
Simulated annealing algorithm
AISI316L stainless steel

ABSTRACT

Pulsed laser welding is a powerful technique especially suitable for joining thin sheet metals. In this study, based on experimental data, pulsed laser welding of thin AISI316L austenitic stainless steel sheet has been modeled and optimized. The experimental data required for modeling are gathered as per Central Composite Design matrix in Response Surface Methodology (RSM) with full replication of 31 runs. Ultimate Tensile Strength (UTS) is considered as the main quality measure in laser welding. Furthermore, the important process parameters including peak power, pulse duration, pulse frequency and welding speed are selected as input process parameters. The relation between input parameters and the output response is established via full quadratic response surface regression with confidence level of 95%. The adequacy of the regression model was verified using Analysis of Variance technique results. The main effects of each factor and the interactions effects with other factors were analyzed graphically in contour and surface plot. Next, to maximum joint UTS, the best combinations of parameters levels were specified using RSM. Moreover, the mathematical model is implanted into a Simulated Annealing (SA) optimization algorithm to determine the optimal values of process parameters. The results obtained by both SA and RSM optimization techniques are in good agreement. The optimal parameters settings for peak power of 1800 W, pulse duration of 4.5 ms, frequency of 4.2 Hz and welding speed of 0.5 mm/s would result in a welded joint with 96% of the base metal UTS. Computational results clearly demonstrate that the proposed modeling and optimization procedures perform quite well for pulsed laser welding process.

1. Introduction

Because of high strength, good corrosion resistance and flexibility to shape, thin stainless steel sheets have wide applications in various industries. Fabrication of such thin sheets, however, is challenging and requires appropriate selection of joining process. Improper joining processes may result in such defects as burn through or incomplete fusion joints that base metal dose not melt properly and lead to have a weak joint. These defects may be caused by extra or insufficient heat input respectively [1–3]. In addition, Adjustment the proper input parameters base on trial and error involve much more time and cost. So selecting the appropriate welding method and adjustment the input parameters lead to have a suitable heat input with acceptable penetration.

In this regard, pulsed Nd:YAG laser welding is one of the few techniques suitable for joining thin sheet metals. Small heat affected zone (HAZ), low heat input per unit volume, high degree of automation and high welding speed are the merits of laser welding technology [4,5].

There is a wide body of research for laser welding and its diverse applications. Balasubramanian modeled the laser beam welding of AISI304 stainless steel sheets with thickness of 1.6 mm butt joint using neural Networks. Laser power, welding speed and beam incident angle are as the input parameters. Also, depth of penetration and bead width are considered as output parameters [6].

Ragavendran et al. [7] successfully modeled and optimized the weld section in the hybrid laser-TIG welding AISI316L Steel with thickness of 5.6 mm. Laser power, pulse frequency and pulse duration are the input parameters setting of laser welding and weld bead width, weld cross-sectional area and depth of penetration are the outputs of optimization.

Cao et al. [8] optimized the process parameters of laser welding on AISI 316L sheet with thickness of 3 mm. The input process parameters are power, welding speed and the flux density of mag-

* Corresponding author.
E-mail address: kolahan@um.ac.ir (F. Kolahan).

https://doi.org/10.1016/j.optlastec.2017.12.042
0030-3992/

netic field. The methods of optimization are combining RBFNN and GA.

Jiang et al. [9] optimized the laser welding process parameters of stainless steel 316L with thickness of 3 mm using FEM, Kriging and NSGA-II. The process parameters are power, welding speed and laser focal position. Also the outputs parameters are bead width and depth of penetration.

With regards to these literature related to statistic modeling and parameter optimization of pulsed laser welding, the thickness of AISI 316L sheets were relatively thick and the studies that optimized the ultra thin sheets of stainless steel 316L are limited. So in this paper the modeling and optimization of pulsed laser welding process is done in austenitic AISI 316L thin sheets with 0.8 mm thickness. Also, studies that have been investigated on five input parameters as power, frequency, pulse duration, welding speed and beam spot size (focal position) simultaneously were not seen. So, in this study, all 5 mentioned input parameters have been considered.

Computer simulations and mathematical modeling are promising approaches to establish the relation between input process parameters and the process output characteristics. To develop an accurate model for the process under study, a set of experimental input–output data is usually required. These data may be gathered based on design of experiment (DOE) tables.

One of the best DOE that are widely used by researchers is Response surface methodology [10,11]. After creating the mathematical model, obtaining the optimal parameters to have a sufficient mechanical property such as ultimate tensile strength is great interest in industrial application [12,13]. Also nowadays, the meta-heuristic algorithms like simulated annealing is a precise method to optimize the objective function in welding [14].

In this study, response surface methodology (RSM) is employed to establish the mathematical relations between the important laser welding process parameters and the joint mechanical strength. In this research, peak power (P_P), pulse duration (Δt), pulse frequency (fr) and welding speed (V) are considered as the most prominent input parameters of the pulsed laser welding. Also, Ultimate Tensile Strength (UTS) is used as the measure of the joint mechanical property. A 4-factor, 5-level Central Composite Design (CCD) matrix with 31 experiments is selected to generate the experimental data.

For maximum joint tensile strength, optimal process parameters settings are determined using desirability functions of RSM [15]. Optimal settings are also specified using Meta heuristic search procedure. For this, a computer code in Matlab v2016 Software is prepared in which the regression model is embedded into a Simulated Annealing (SA) algorithm. Optimization results are verified against experiment.

2. Experimental procedures

2.1. Material and equipment

Experimental was carried out on AISI316L stainless steel sheets with 0.8 mm thickness cut into 55 mm × 30 mm specimens. AISI316L stainless steel with at least 11% chromium provides the shiny appearance and superior corrosion resistance. This alloy can maintain its mechanical and physical properties in most environmental conditions. Such properties make this alloy very desirable in marine and chemical industries. The major chemical composition and mechanical/physical properties of this alloy are listed in Table 1.

Experimental tests, with butt welding configuration, were carried out on a 1.064 μm wavelength Trumpf HL54p solid state pulsed Nd:YAG machine. The characteristic of this welding machine is 70 W average laser power, peak power 5KW, pulse duration range 0.5–20 ms, frequency range 0.1–20 Hz and spot diameter range 0.3–2 mm. The welding apparatus and its associated laser generating device are illustrated in Fig. 1.

In all tests, pure (99.9%) argon with flow rate of 10lit/min was flowed in the specimens as the shielding gas in order to prevent the oxidation with an incident angle of 45° in Fig. 2. Furthermore, the incident angle of 90 degrees with respect to the weld line was used to shot the laser beam. Prior to each test, sheet edges were prepared by grinding operation. Then each pair of sheets were fixed in the clamping fixture and tack welded in a butt joint configuration along their 30 mm width of sheets (Fig. 2).

2.2. Process input variables and their levels

The most five important processes parameters in pulsed laser welding are peak power, pulse frequency, pulse duration, beam spot size and welding speed [16–19]. First, in order to decrease the experimental tests, the beam spot size was independently investigated to other variables. Regarding that, some limited tests were carried out by changing the beam spot size from 0.3 mm to 0.5 mm and 0.7 mm while other parameters (i.e., peak power 1850 W, pulse duration 4.5 ms, frequency 4.5 HZ and welding speed 0.4 mm/s) were kept constant (Fig. 3). The results show that with increase in beam spot size, the heat input will be lessened and it, consequently, causes smaller penetration. Thus, beam spot size of 0.3 mm was considered as constant parameter in the process and therefore, others were considered as input variables in this study. Furthermore, the UTS, an important measure of the joint mechanical property, was selected as a process output response [5,17,19,20].

In order to identify the feasible working ranges of the four input variables, preliminary tests were carried out and the quality of weldment like visual appearance and penetration were observed. According to these tests results, the proper ranges of process parameter were determined. These along with their intermediate levels (five levels in total) are listed in Table 2.

Experimental tests have been carried out using various combinations of the parameters levels as given by the selected Design of Experiment (DOE) matrix.

2.3. Design of experiment (DOE) matrix and test results

Design of experiments (DOE) approach is a set of tools that, with limited number of tests, helps to identify the influence of each process parameter and establish the relationships between input parameters and output responses [21]. Among various DOE procedures, in Response Surface Methodology (RSM), minimum number of experimental runs are needed and also are an effective technique most suitable for the cases in which the approximate values of the optimal process inputs are known [22]. One of the most advantages of RSM is that, it will analyze the interaction between various welding process parameters and output responses. Furthermore, the response can be studied as contour plots or three dimensional response surface plots.

Central Composite Design (CCD) is the most well-know design methodology within RSM. CCDs are arranged around the central points with several replications of 0 levels. In the recent years, the CCD is very useful for applying the DOE [7,23,24].

In this study, using Minitab® V17 software, a CCD matrix with full replication is generated. The 31 experiments include full 2^4 factorial design (16 tests), seven central and eight star points. This design involves the full quadratic effects consisting of linear, square and two-way interactions on the response surface.

Table 1
Chemical compositions and mechanical/physical property of AISI316L alloy used.

Element	C	Si	Mn	Cr	Mo	Ni	Cu	Fe
Weight (%)	0.029	0.41	1.51	17.13	2.01	10.75	0.38	Balance
Mechanical property					Physical property			
Ultimate tensile strength			630 Mpa		Density		7990 kg/m^3	
Yield stress			270 Mpa		Specific heat		0.5 kJ/kg K	
Hardness			145 VH		Thermal conductivity		16.2 W/m K	
Elongation			57%					

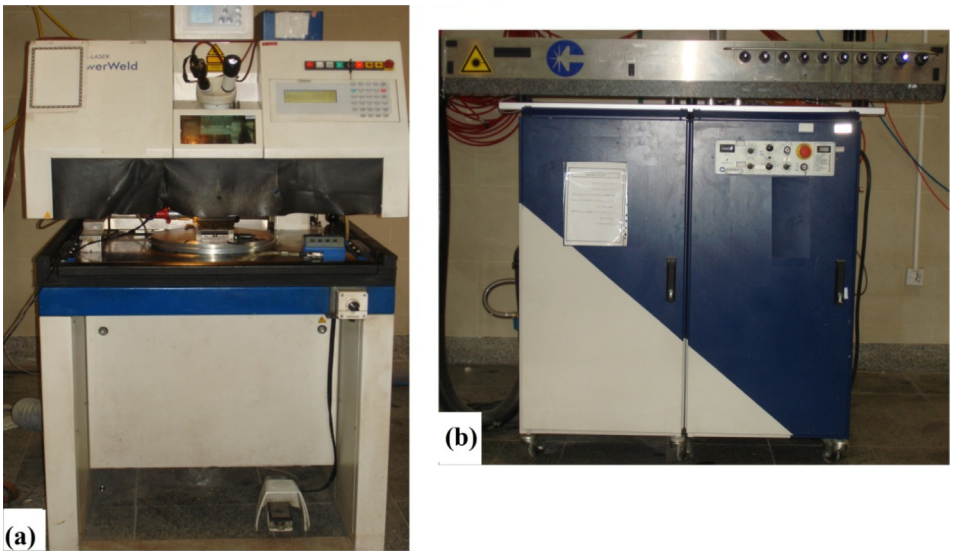

Fig. 1. Trumpf Nd:YAG laser welding system, (a) laser welding machine; (b) laser generating device.

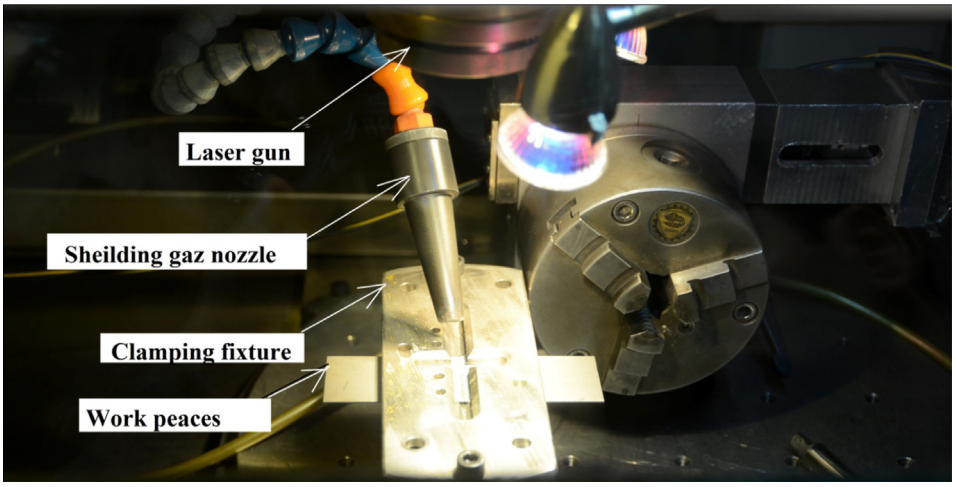

Fig. 2. Experimental setup.

After welding, the tensile strength test samples, as shown in Fig. 4, were cut by wirecut operation according to the ASTM E8 standard [25].

The ultimate tensile strength (strength at fracture) of the 31 samples were then determined using the GOTECH-TCS2000 universal testing machine at speed of 0.5 mm/min according to ASTM E8 standard [25]. Fig. 5 illustrates the specimens after performing UTS tests.

Table 3 shows laser welding parameters levels and the measured UTS (Mpa) for each experiment. As reported in this Table, the maximum and minimum UTSs of 603 Mpa and 389.6 Mpa correspond to test numbers 14 and 9, respectively.

The metallographic process consists of mounting and electro etching is done. Then, with Olympus BX51M Microscope in 100 zoom optic, cross sections of these samples are dimensioned as demonstrated in Fig. 6. While Fig. 6a shows a good welded joint,

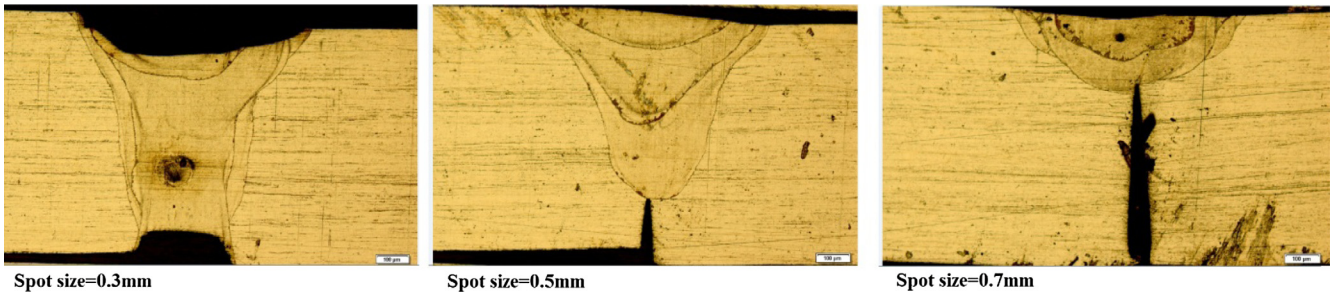

Fig. 3. Effect on beam spot size on penetration.

Table 2
Pulsed Nd:YAG laser beam welding process parameters and their limits.

Parameters	Units	Symbols	Limits				
			−2	−1	0	+1	+2
Peak power	W	P_p	1650	1700	1750	1800	1850
Pulse duration	ms	Δt	3.5	4	4.5	5	5.5
Pulse frequency	Hz	fr	3	3.5	4	4.5	5
Welding Speed	mm/s	V	0.2	0.3	0.4	0.5	0.6

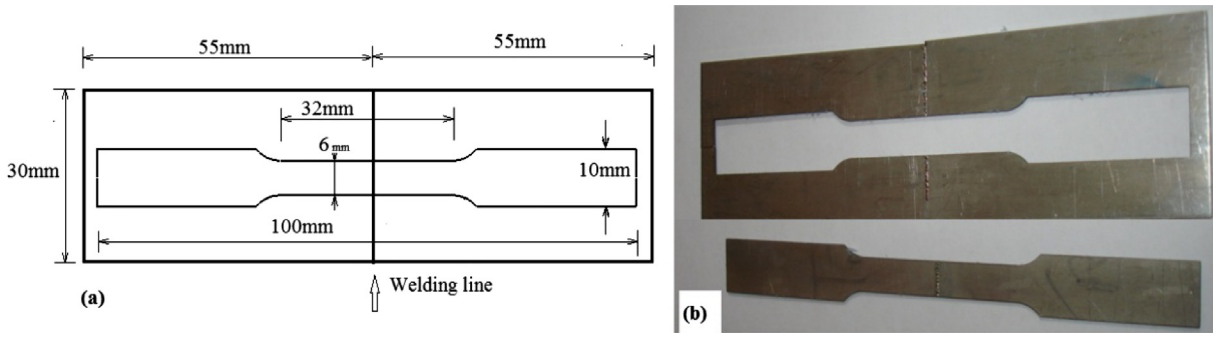

Fig. 4. Stainless steel alloy thin sheets were butt welded and wirecuted as a standard sample for tensile test.

the inadequate weld penetration illustrated in Fig. 6b is the main reason for low tensile strength of the sample.

3. Modeling of the pulsed laser welding

3.1. Developing the regression model

The RSM uses the 31 sets of experimental to establish a second order polynomial function describing the correlations between the joint UTS and the four welding input parameters, namely peak power, pulse duration, pulse frequency and welding speed. The general form of second order polynomial equation is provided as follow (Eq. (1)) [22]:

$$UTS = b_0 + \sum_{i=1}^{k} c_i X_i + \sum_{i=1}^{k} d_{iX_i^2} + \sum_{i<j}\sum_{i=1}^{k} e_{ijX_iX_j} + \varepsilon \quad (1)$$

where b_0 is the response of the central point and c_i, d_i and e_{ij} are the coefficients of linear, squared and interaction terms in the regression function. The method of least squares is applied to estimate the coefficients in the approximating polynomial [22].

ANOVA method is utilized to investigate the significance of the mathematical model. Thus, Confidence level is considered in 95%. In this regard, if some terms became insignificant, they eliminated and the regression recalculated. This process was continued until all terms became significant. In Table 4 the final ANOVA analyses with eliminating the insignificant term (the interaction between peak power and welding speed) is shown.

With regards to Table 4, for the final ANOVA analysis, all remaining terms have P-values of less than 0.05 and hence satisfy the required confidence level of 95%. In addition, the value of R^2 = 97.99%, R^2 (adj) = 96.46% and R^2(pre) = 91.43% indicated the high correlation between experimental values and predicted values from developed model. Furthermore, the amount of $F_{0.05,13,17} = 2.35$ is smaller than that of obtained in the model.

Finally with adequacy of the model, the regression with a second order polynomial equation predicted the response surface "UTS" according to Eq. (2) by using of least square method in RSM.

$$\begin{aligned} UTS = {} & 584.73 + 26.64P_P + 14.23\Delta t + 19.03Fr + 18.83V \\ & - 11.28P_P^2 - 17.09\Delta t^2 - 25.34Fr^2 - 20.91V^2 - 9.15P_P \\ & \times \Delta t - 11.56P_P \times Fr - 35.69\Delta t \times Fr + 12.03\Delta t \times V \\ & + 18.96Fr \times V \end{aligned} \quad (2)$$

Also, as shown in Fig. 7, the validity of the model was surveyed by residual plots for UTS response. Like, in normal probability plot, the residuals were located in the straight line. Furthermore, in Histogram plot, the normality distribution was seen. So the validity of model was proven.

The ANOVA results and residual plots prove the adequacy of the proposed RSM model for pulsed laser welding process. Therefore, this model may be used for further analysis.

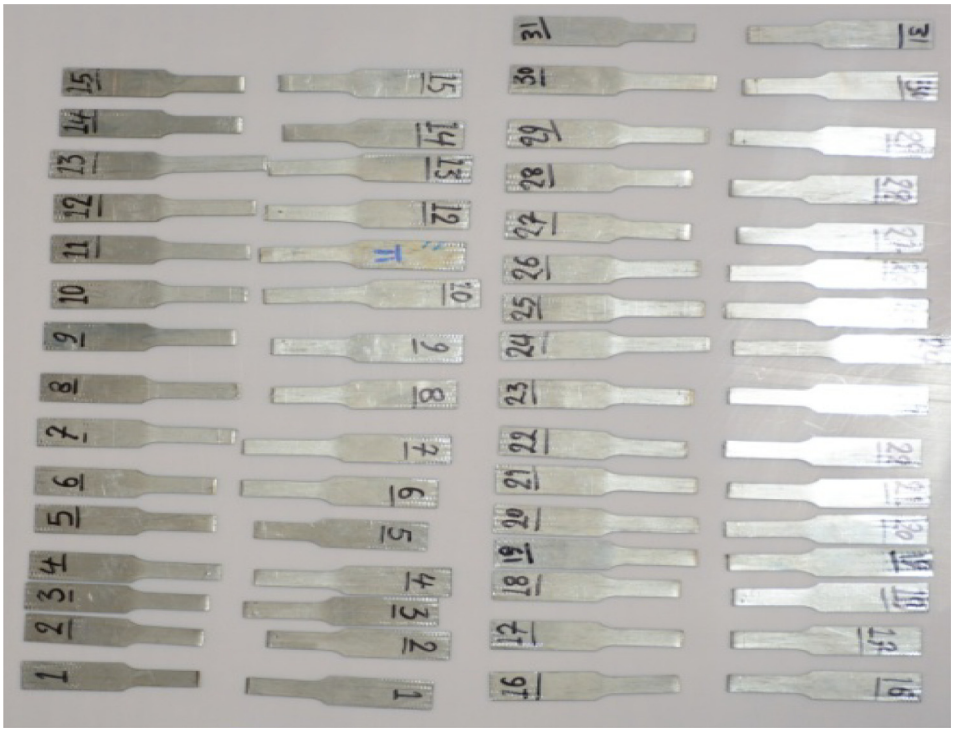

Fig. 5. 31 specimens were carried out under tension with tensile strength test machine.

Table 3
31 specimens were carried out under tension with tensile strength test machine.

Experimental details					Response
Exp. No.	Factors				
	P_P	Δt	fr	V	UTS(Mpa)
1	−1	−1	−1	−1	412.5
2	+1	−1	−1	−1	494.8
3	−1	+1	−1	−1	506.7
4	+1	+1	−1	−1	572.9
5	−1	−1	+1	−1	500.0
6	+1	−1	+1	−1	556.3
7	−1	+1	+1	−1	456.9
8	+1	+1	+1	−1	461.5
9	−1	−1	−1	+1	389.6
10	+1	−1	−1	+1	483.3
11	−1	+1	−1	+1	525.0
12	+1	+1	−1	+1	591.7
13	−1	−1	+1	+1	545.8
14	+1	−1	+1	+1	603.1
15	−1	+1	+1	+1	563.1
16	+1	+1	+1	+1	568.8
17	−2	0	0	0	479.2
18	2	0	0	0	582.5
19	0	−2	0	0	487.5
20	0	2	0	0	527.7
21	0	0	−2	0	430.2
22	0	0	+2	0	519.0
23	0	0	0	−2	456.5
24	0	0	0	+2	528.1
25	0	0	0	0	583.3
26	0	0	0	0	594.4
27	0	0	0	0	580.2
28	0	0	0	0	597.7
29	0	0	0	0	572.9
30	0	0	0	0	585.4
31	0	0	0	0	579.2

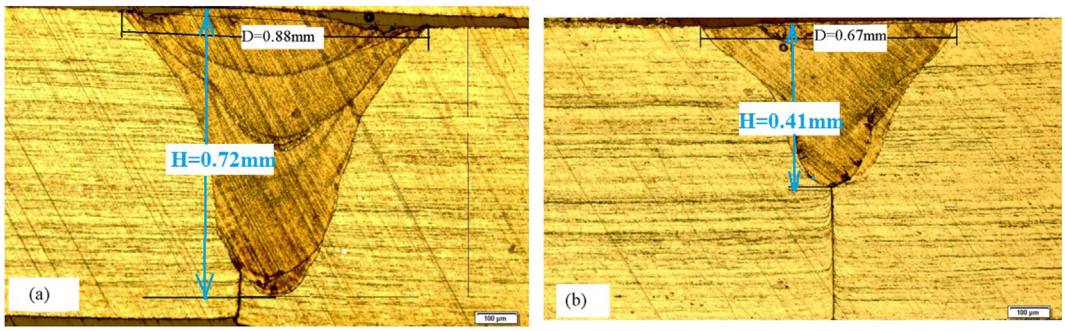

Fig. 6. Weld section dimensions: (a) test number 14 and (b) test number 9.

Table 4
Analysis of variance test results for checking adequacy of the developed model.

Source	DF	Adj SS	Adj MS	F-value	P-value
Model	13	104,605	8046.6	63.90	<0.001
Linear	4	39,096	9774.1	77.61	<0.001
P_P	1	17,035	17034.7	135.27	<0.001
Δt	1	4862	4862.1	38.61	<0.001
fr	1	8687	8686.8	68.98	<0.001
V	1	8513	8512.7	67.60	<0.001
Square	4	33,586	8396.5	66.68	<0.001
$P_P \times P_P$	1	3636	3635.8	28.87	<0.001
$\Delta t \times \Delta t$	1	8350	8350.3	66.31	<0.001
fr × fr	1	18,359	18359.4	145.79	<0.001
V × V	1	12,507	12506.9	99.32	<0.001
2-way Interaction	5	31,923	6384.6	50.70	<0.001
$P_P \times \Delta t$	1	1340	1339.6	10.64	0.005
$P_P \times$ fr	1	2139	2139.1	16.99	0.001
$\Delta t \times$ fr	1	20,378	20377.6	161.81	<0.001
$\Delta t \times$ V	1	2314	2313.6	18.37	<0.001
fr × V	1	5753	5753.2	45.69	<0.001
Error	17	2141	125.9		
Lack-of-fit	11	1686	153.2	2.02	0.201
Pure error	6	455	75.9		
Total	30	106,746			
S = 11.2219					
R^2 = 97.99%					
$R^2_{(adj)}$ = 96.46%					
$R^2_{(pre)}$ = 91.43%					

3.2. Main effects of factors on UTS

A main effect is present when different levels of a factor affect the response differently. When the line is not horizontal, then there is main effect present. With regards to Fig. 8, there are main effects of process parameters on UTS. As indicated, the main effects of peak power, pulse duration, pulse frequency and welding speed on UTS are 27.7%, 15.5%, 32.2% and 24.4% respectively. Therefore the pulse frequency and peak power are more significant than pulse duration and welding speed, since they may cause higher variations in UTS. Furthermore, the graphs show that with increase of peak power, more energy is transferred, and consequently, lead to have a full penetration and cause to enhance the UTS. But, other three input variables (pulse duration, frequency and welding speed) increase, the UTS at first increase and then decrease [26]. It is suppose that the main reason to decrease the UTS in upper level (+2) of pulse duration and frequency and also in lower levels of welding speed is that excessive heat input is transferred in the work pieces, and consequently, lead to have vaporization instead of welding [10,26]. In addition, in upper level of welding speed (+2), with regards to high welding speed, there is not sufficient time to melt the material and lead to have a welding joints. It is necessary to mention that in main effect plots, for survey of each parameter, provided that the other three parameters are set at their mid-levels.

3.3. Analysis of interactions contour plots and response graphs

One of the most important advantages of CCD is the analyses of interaction effects of process parameters on output responses with studding of interaction contours and 3D surface plots [27]. Also, these contour and plots has the high capability to specify the optimal areas between two factors if exist.

For analyzing the two factors, the other factors must be kept at its central levels. With regards to Fig. 9, the most important interaction effect of two parameters on UTS is shown. As indicated in contour plots, for every four interactions, a central elliptical area is the optimal levels on UTS. Also, it is evident from 3D surface plots that all interaction plots are convex shape. At first in Fig. 9a, the interaction between Peak power and frequency on UTS is analyzed. First, for increase in laser power and frequency, more energy is transferred, and consequently, lead to have a full penetration and higher UTS. But after that, with too much increase in the power and frequency, it lead to have an extra energy in which causes evaporation of the metals and burn-through will be happened, resulting lower UTS [10]. These plots show that for obtaining the optimal areas in UTS, the ranges of peak power must be between 1795 W and 1825 W. In addition, the ranges of pulse frequency must be between 4 Hz and 4.25 Hz. These ranges in the contour plot are the small elliptical areas that specify the UTS is greater than 600 Mpa.

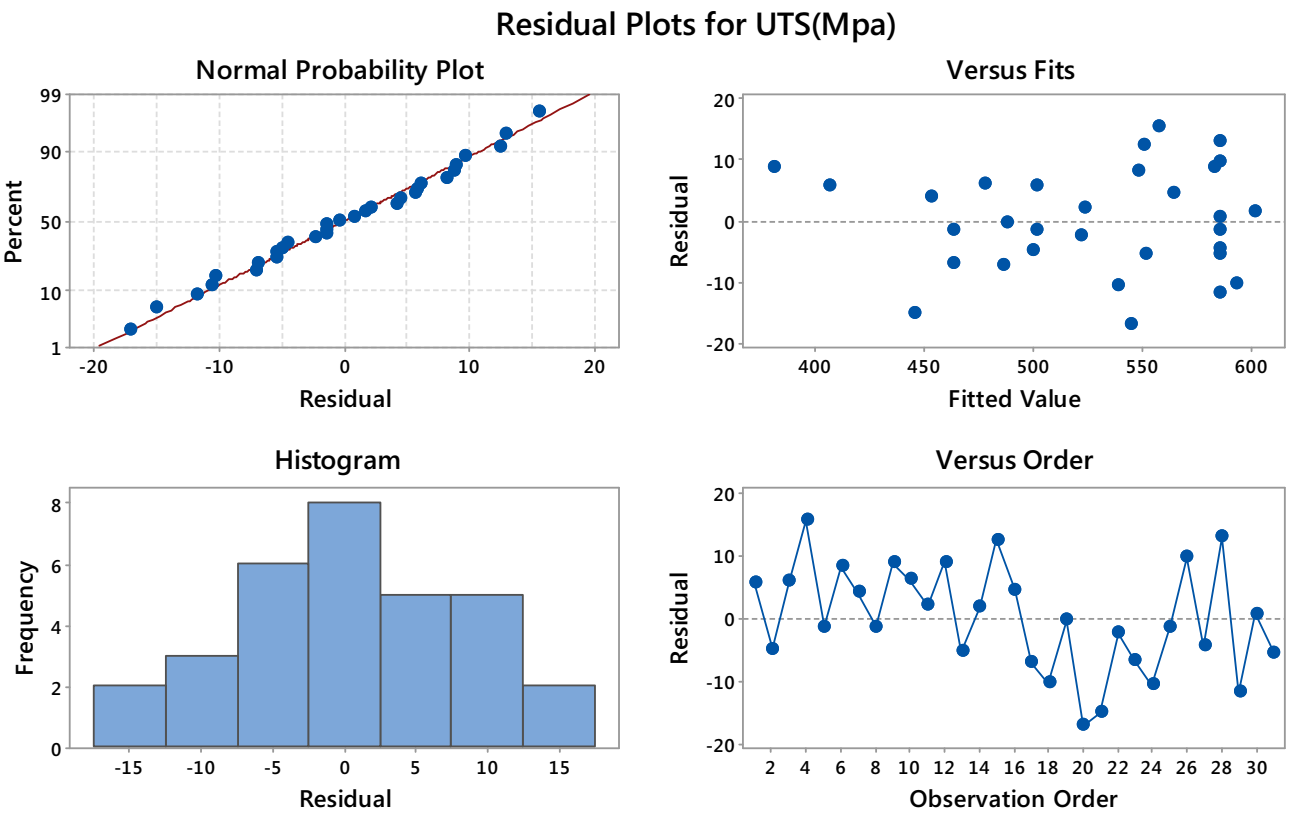

Fig. 7. Residual plots for UTS Response.

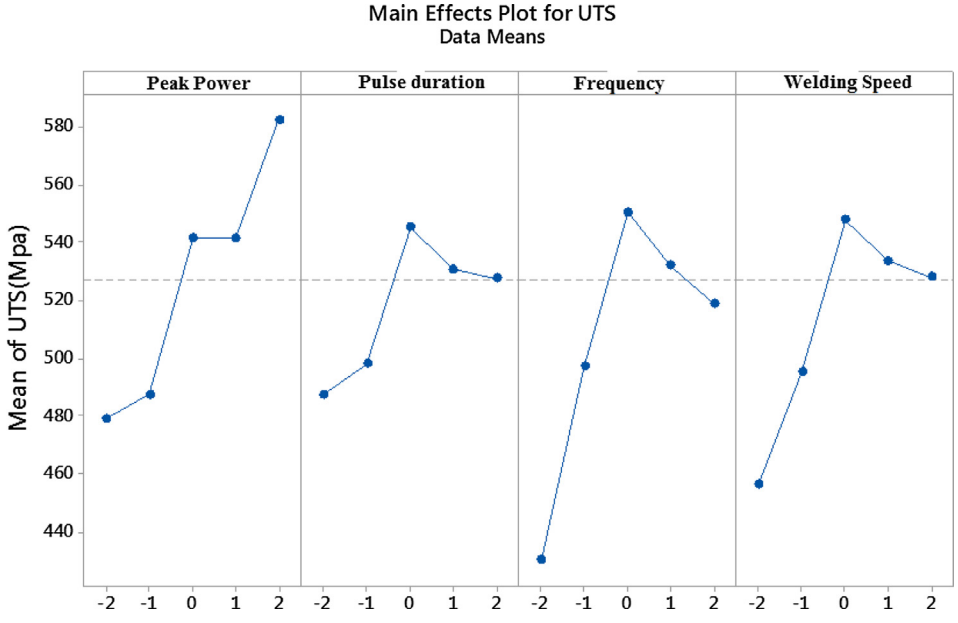

Fig. 8. Main effects of factors on UTS (Mpa).

The next analysis is the interaction effects of pulse duration and pulse frequency on UTS. Therefore, contour and 3D surface plots between them is shown in Fig. 9b. There is a significant interaction between pulse duration and frequency for response surface of UTS. As shown, in lower frequency and pulse duration and also in upper frequency and pulse duration, the UTS are small. Thus, the UTS was enhanced in near central levels of frequency and pulse duration. Hence, a large elliptical area in which UTS is more than 550 Mpa can be seen as well. It is assumed that in lower frequency and pulse duration, the heat input is insufficient and lead to have a low penetration and low UTS. But in near central levels of frequency and pulse duration, the heat input will enhance and lead to have a more

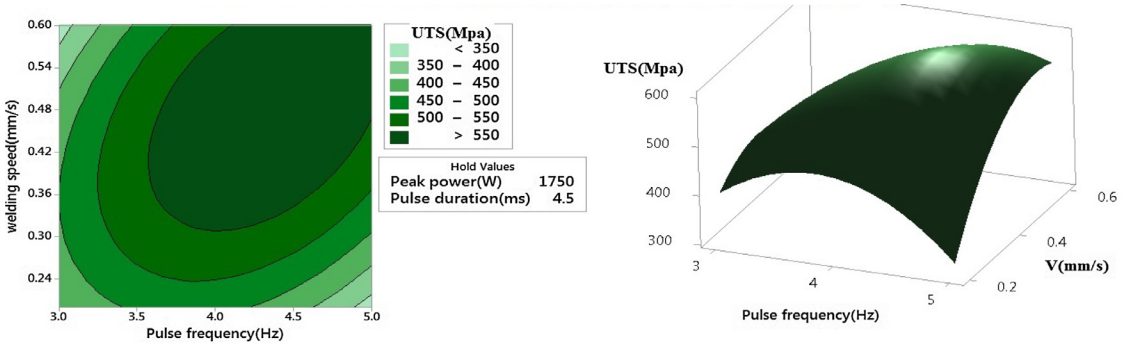

(d) Contour and 3D surface plots between frequency and Welding speed on UTS

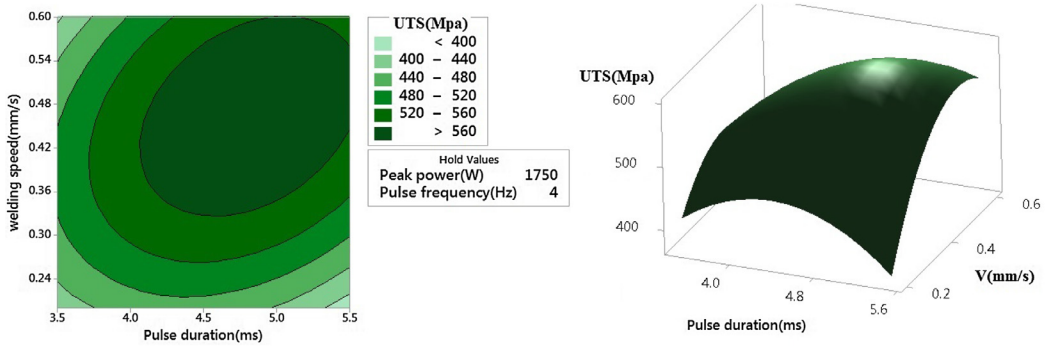

(c) Contour and 3D surface plots between Pulse duration and Welding speed on UTS

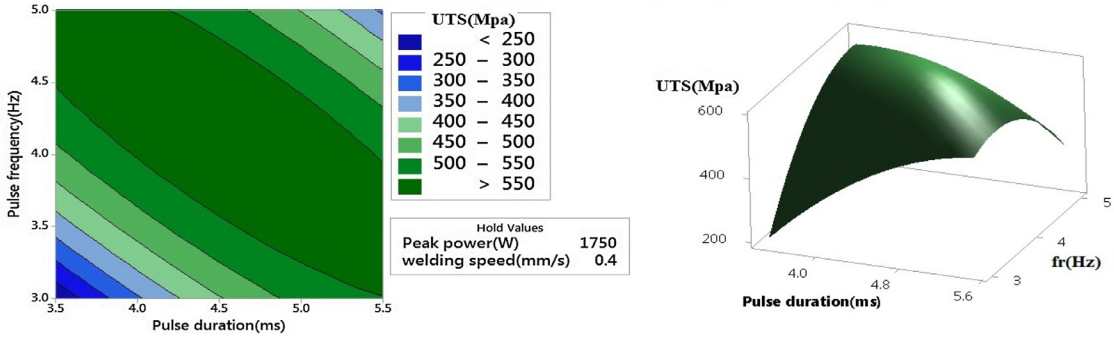

(b) Contour and 3D surface plots between Pulse duration and Frequency on UTS

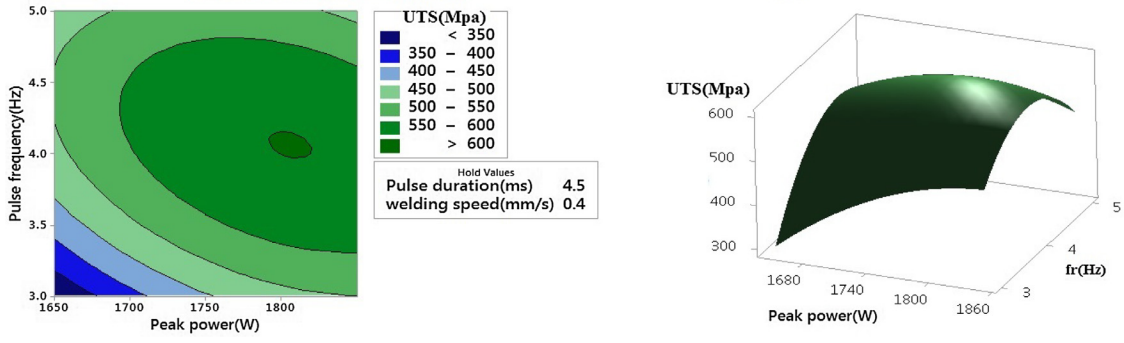

(a) Contour and 3D surface plots between Peak power and frequency on UTS

Fig. 9. Contour and 3D surface plots of the interaction effect of any two parameters on UTS.

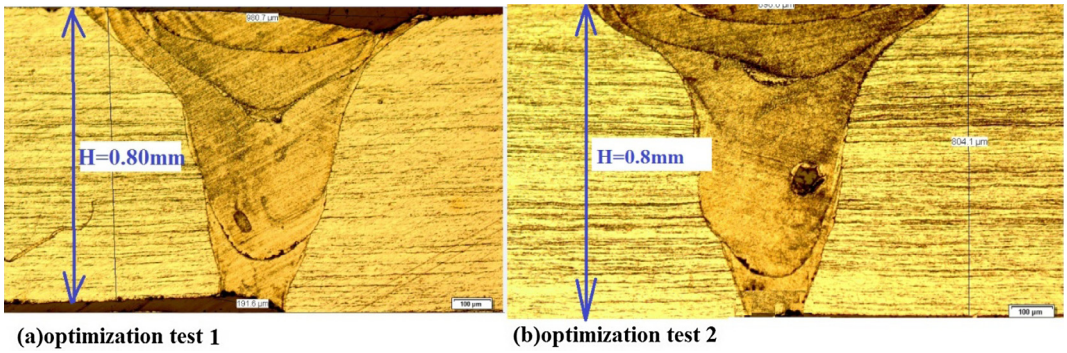

Fig. 10. The weld section dimensions of 2 optimal parameters tests.

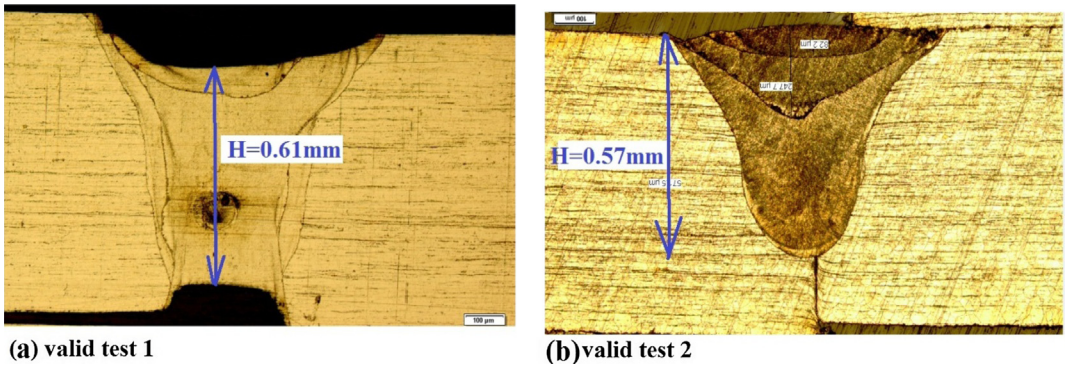

Fig. 11. The weld section dimensions of 2 validation tests.

Table 5
Optimized laser beam welding process parameters.

Parameters	Optimized settings predicted by RSM and SA	Maximum tensile strength (Mpa)		
		Predicted by RSM and SA	Experimental test	
			No. 1	No. 2
Peak power (W)	1800			
Pulse duration (ms)	4.50	608	604.8	609.2
Pulse frequency (Hz)	4.2			
Welding speed (mm/s)	0.5			
			Average = 607 Mpa	

Table 6
Two validation tests results.

Experimental details					Response	
Valid test. No.	Factors				UTS (Mpa) in predicted by regression model	UTS (Mpa) in experimental
	P_P (W)	Δt (ms)	Fr (Hz)	V (mm/s)		
1	1850	4.5	4.5	0.4	563.5	551.2
2	1700	4	4	0.4	506.3	498.5

penetration and UTS. Because of small thickness of samples, if the frequency and pulse duration increase excessively, heat input will increase and consequently burn-through could be happened.

Finally, the effects of pulse duration, welding speed as well as the interaction effects of pulse frequency and welding speed on UTS was analyzed and shown in Fig. 9c and d. For both of them, large elliptical areas were specified for obtaining the maximum UTS [26]. In addition, the ranges of these parameters are around 4.2–5.5 ms, 0.32–0.60 (mm/s) and 3.6–5 (Hz). Also, both plots illustrate that lower welding speed (0.2–0.3 mm/s) led to have a concave shape of top surface owing to the excessive heat input [10] and consequently, have lower penetration and UTS. Another reason

for UTS decrease (in low welding speed) can be related to excessive heat input, followed by slow cooling rate and consequent grain coarsening in the molten pool [12].

With regards to have 4 different optimal areas, an optimization process is needed to specify the accurate optimal levels.

4. Optimization

In this section, optimal values of laser welding process parameters have been determined to maximize the UTS of the welded joint. Thus, in this paper, the optimal parameters settings are predicted and compared using two different approaches namely, Simulated Annealing (SA) algorithm and desirability function of RSM.

In SA optimizing approach, at first, the mathematical model (Eq. (2)) as the objective function is implanted into a Simulated Annealing (SA) optimization algorithm. Then, the starting point is specified as peak power of 1650 W, pulse duration of 3.5 ms, pulse frequency of 3 Hz and welding speed of 0.2 mm/s. the "max interaction" bounds the number of iterations that takes in the algorithm. In this optimization, the "max interaction" is considered as 1000 in order to reduce the calculation time with acceptable precise. Also, the annealing function is selected as "Boltzmann-A nnealing". Finally, the initial temperature is specified as 80 °C and the algorithm is done.

In addition to the above mentioned algorithm, optimal values of process parameters may be calculated using the desirability function of RSM in Minitab Software. Optimizations results summarized in Table 5, indicating both SA and RSM have come up with the same set of process parameters values and both could predict the same UTS. In the table, the second column reports the optimal settings calculated by both RSM and SA algorithm. In order to evaluate the correctitude of the optimal levels of parameters that predicted by RSM and SA, two actual test was done. The third column of Table 5 corresponds to the predicted and the experimentally obtained UTS for welded joint made by the optimal settings. With regards to values of UTS in optimal condition (604.8 Mpa and 609.2 Mpa) and full penetration as indicated in Fig. 10, near 96% maximum ultimate tensile strength of base metal was obtained. These values are very close to the UTS of the base metal (630 Mpa). Also to validate the regression model, two experiments were done as indicated in Fig. 11. The input parameters and results from validation test are reported in Table 6. With comparing the UTS from experimental tests and predicted values in Tables 5 and 6, the optimization and validation tests are very good compatibility with experimental data and therefore demonstrate the effectiveness of the proposed approach. The proposed model can likely account as a accurate prediction for the ultimate tensile strength values in pulsed laser welding of thin AISI316L sheets.

5. Conclusions

The experimental investigation on pulsed Nd:YAG laser welding in thin sheet plates AISI316L are analyzed by statistic Minitab software. Mathematical modeling and optimization of the laser welding process are the most important parts of the current paper. The objective of optimization procedure is to determine the best set of process variables levels for obtaining the maximum ultimate tensile strength. The significant items were concluded as following:

1. A mathematical model was developed in which the UTS can be predicted with an acceptable accuracy. In fact, observing the residual plots and surveying the correlation coefficients (R^2 = 97.99%, R^2(adj) = 96.46% and R^2(pre) = 91.43%) prove the claim. Also. Two validation tests prove the reliability of the model.
2. Main effect in frequency and peak power are more significant with effects of 32.2% and 27.7% than pulse duration and welding speed.
3. The RSM is a good statistic method to analyze the interaction between factors in this study.
4. The optimization in two methods of RSM and SA was done. Results indicate that both the SA and RSM methods are very good compatibility with experimental results.
5. An average Maximum UTS of 607 Mpa with near 96% UTS in base metal (630 Mpa) was obtained by setting the optimized process parameters.

The results and validation tests indicate that the proposed modeling and optimization approaches are quite capable of predicting the quality measure responses in pulsed laser welding of thin steel sheet. The pulsed laser welding is shown to be a very suitable method for joining thin sheet metals, as it can produce joints with same strength as the base metal.

References

[1] X. Cao, M. Jahazi, Effect of welding speed on butt joint quality of Ti–6Al–4V alloy welded using a high-power Nd: YAG laser, Opt. Lasers Eng. 47 (11) (2009) 1231–1241.

[2] D. Min, J. Shen, S. Lai, J. Chen, Effect of heat input on the microstructure and mechanical properties of tungsten inert gas arc butt-welded AZ61 magnesium alloy plates, Mater. Char. 60 (12) (2009) 1583–1590.

[3] A.Y. Kaitanov, A. Ozersky, A. Zabelin, V. Kislov, Static and fatigue strengths of laser welded overlap joints with controlled penetration, in: Proc. SPIE, 2002.

[4] X.-L. Gao, L.-J. Zhang, J. Liu, J.-X. Zhang, A comparative study of pulsed Nd: YAG laser welding and TIG welding of thin Ti6Al4V titanium alloy plate, Mater. Sci. Eng. 559 (2013) 14–21.

[5] V.A. Ventrella, J.R. Berretta, W. de Rossi, Micro welding of Ni-based alloy Monel 400 thin foil by pulsed Nd: YAG laser, Phys. Procedia 12 (2011) 347–354.

[6] K.R. Balasubramanian, G. Buvanashekaran, K. Sankaranarayanasamy, Modeling of laser beam welding of stainless steel sheet butt joint using neural networks, CIRP J. Manuf. Sci. Technol. 3 (2010) 80–84.

[7] M. Ragavendran, N. Chandrasekhar, R. Ravikumar, R. Saxena, M. Vasudevan, A. Bhaduri, Optimization of hybrid laser–TIG welding of 316LN steel using response surface methodology (RSM), Opt. Lasers Eng. 94 (2017) 27–36.

[8] L. Cao, Y. Yang, P. Jiang, Q. Zhou, G. Mi, Z. Gao, Y. Rong, C. Wang, Optimization of processing parameters of AISI 316L laser welding influenced by external magnetic field combining RBFNN and GA, Results Phys. 7 (2017) 1329–1338.

[9] P. Jiang, C. Wang, Q. Zhou, X. Shao, L. Shu, X. Li, Optimization of laser welding process parameters of stainless steel 316L using FEM, Krig. NSGA-II. Adv. Eng. Software 99 (2016) 147–160.

[10] Y. Zhao, Y. Zhang, W. Hu, X. Lai, Optimization of laser welding thin-gage galvanized steel via response surface methodology, Opt. Lasers Eng. 50 (9) (2012) 1267–1273.

[11] U. Reisgen, M. Schleser, O. Mokrov, E. Ahmed, Optimization of laser welding of DP/TRIP steel sheets using statistical approach, Opt. Laser Technol. 44 (1) (2012) 255–262.

[12] G. Padmanaban, V. Balasubramanian, Optimization of laser beam welding process parameters to attain maximum tensile strength in AZ31B magnesium alloy, Opt. Laser Technol. 42 (8) (2010) 1253–1260.

[13] L.K. Pan, C.C. Wang, Y.C. Hsiao, K.C. Ho, Optimization of Nd:YAG laser welding onto magnesium alloy via Taguchi analysis, Optics & Laser Opt. Laser Technol. 37 (1) (2005) 33–42.

[14] R. Padmanaban, V. Balusamy, V. Saikrishna, K.G. Niranthar, Simulated annealing based parameter optimization for friction stir welding of dissimilar aluminum alloys, Procedia Eng. 97 (2014) 864–870.

[15] N.R. Costa, J. Lourenço, Z.L. Pereira, Desirability function approach: a review and performance evaluation in adverse conditions, Chemom. Intell. Lab. Syst. 107 (2) (2011) 234–244.

[16] W. Han, J. Byeon, K. Park, Welding characteristics of the Inconel plate using a pulsed Nd: YAG laser beam, J. Mater. Process Technol. 113 (1) (2001) 234–237.

[17] P. Sathiya, K. Panneerselvam, M.A. Jaleel, Optimization of laser welding process parameters for super austenitic stainless steel using artificial neural networks and genetic algorithm, Mater. Des. 36 (2012) 490–498.

[18] Q. Han, D. Kim, D. Kim, H. Lee, N. Kim, Laser pulsed welding in thin sheets of Zircaloy-4, J. Mater. Process Technol. 212 (5) (2012) 1116–1122.

[19] N. Sivagurumanikandan, S. Saravanan, G.S. Kumar, S. Raju, K. Raghukandan, Prediction and optimization of process parameters to enhance the tensile strength of Nd:YAG laser welded super duplex stainless steel, Optik 157 (2018) 833–840.

[20] N. Xiansheng, Z. Zhenggan, W. Xiongwei, L. Luming, The use of Taguchi method to optimize the laser welding of sealing neuro-stimulator, Opt. Lasers Eng. 49 (3) (2011) 297–304.

[21] M. Azadi Moghaddam, R. Golmezergi, F. Kolahan, Multi-variable measurements and optimization of GMAW parameters for API-X42 steel alloy using a hybrid BPNN–PSO approach, Measurement 92 (2016) 279–287.
[22] D.C. Montgomery, Design and analysis of experiments, John Wiley & Sons, 2008.
[23] H. Mostaan, M. Shamanian, S. Monirvaghefi, P. Behjati, J. Szpunar, Magnetic properties assessment of laser welded ultra-thin Fe–Co–V foils, J Alloys Compd. 615 (2014) 56–64.
[24] H. Mostaan, M. Shamanian, S. Monirvaghefi, P. Behjati, J. Szpunar, J. Sherafati, Electron beam assisted joining of nanograin-sized Fe–Co–V magnetic foils: study and optimization of magnetic properties of weld joints, Vacuum 109 (2014) 148–156.
[25] Standard ASTM , Standard Test Methods for Tension Testing of Metallic Materials, Annu Book ASTM Standards 3 (2004) 57–72.
[26] H. Mostaan, M. Shamanian, S. Hasani, M. Safari, J. Szpunar, Nd: YAG laser micro-welding of ultra-thin FeCo–V magnetic alloy: optimization of weld strength, Trans. Nonferrous Met. Soc. China 27 (8) (2017) 1735–1746.
[27] R.A. Johnson, I. Miller, J. Freund, Probability and Statistics for Engineers, Miller & Freund's, 2000, pp. 546–554.